Journal of Inorganic and General Chemistry
ZAAC
Zeitschrift für anorganische und allgemeine Chemie
www.zaac.wiley-vch.de
RESEARCH ARTICLE
DOI: 10.1002/zaac.202200062

Large and Small Solids: A Journey Through Inorganic Chemistry

Claus Feldmann*[a]

On the occasion of the special issue to celebrate 130 years of ZAAC.

On the occasion to celebrate 130 years of *ZAAC*, we summarize about 20 years of our journey through inorganic chemistry with *"large"* solids (single-crystalline compounds) and *"small"* solids (nanomaterials). This includes the syntheses (water, polyols, ethers, liquid ammonia, ionic liquids) and structures (crystal structure and nanostructure) as well as the respective properties (especially bonding and stability, luminescence, catalysis and photocatalysis, imaging and drug delivery). Specific examples of large and small solids comprise metal-oxide nanoparticles, base-metal nanoparticles, hollow nanospheres, polyhalides and halogen-rich metal halides, carbonyl and cluster compounds, as well as inorganic-organic hybrid nanoparticles.

1. Introduction

130 years of inorganic chemistry is a period, in which enormous scientific achievements have been made in chemistry and the related disciplines. Our journey is significantly shorter and started in 1992 with a very first publication soon after the diploma thesis in – how can it be any different – the *ZAAC*.[1] After PhD thesis, certain time in industry and habilitation, the first publication as a newly appointed professor in 2004 was – of course – again in the *ZAAC*.[2] Over the years, *ZAAC* has been a continuous companion with the most recent publication – namely this one – in this journal. After the honorable request to contribute to the special issue of *ZAAC* on the occasion of its 130th anniversary, the immediate question was what could be the subject of such a contribution? With this research report, we try to answer with a bit of our journey through inorganic chemistry.

Starting from roots in solid-state chemistry and industrial chemistry, our journey through inorganic chemistry is still focused on new solid compounds and their properties but developed from classic solid-state chemistry to liquid-phase synthesis and nanomaterials, so that our path now could be designated as liquid-phase synthesis of large (single crystalline) and small (nanosized) solids. With this general focus, different types of liquid-phase syntheses (including water, polyols, ethers, liquid ammonia, ionic liquids) have been established to obtain different types of compounds (ranging from base-metal nanoparticles via hollow nanospheres to polyhalides and halogen-rich metal halides as well as carbonyl and cluster compounds). In regard to different types of compounds, different types of properties, ranging from crystal structure and nanostructure via luminescence and photo-/catalysis to drug delivery and biomedical application have been addressed. Some selected results are illustrated in the following.

[a] *Prof. Dr. C. Feldmann*
Institut für Anorganische Chemie
Karlsruhe Institute of Technology (KIT)
Engesserstraße 15, D-76131 Karlsruhe (Germany)
Phone: (+)49-721-60842855
E-mail: claus.feldmann@kit.edu
Homepage: http://www.aoc.kit.edu

2. Results and discussion

2.1. Polyol-mediated synthesis and metal oxide nanoparticles

The so-called polyol synthesis was firstly described by *Fievet*, *Lagier*, and *Figlarz* in 1989[3] and introduced for the synthesis of metal particles such as Co, Ni or Cu. Accordingly, a high-boiling, multivalent alcohol – the polyol – serves as solvent of the starting materials (e.g., metal chlorides, metal acetates), reducing agent, and colloidally stabilizing dispersant for the as-prepared metal nanoparticles, which are highly uniform in size and predominately obtainable in a size range of 50 to 500 nm.[4] The reducing power depends on the polyol (glycerol used most often) and the temperature, which gives good control of nucleation and growth. Based on Fievet's pioneering work, we could expand the polyol method as a general access to metal-oxide nanoparticles.[5] Thus, crystalline metal oxides in a size range of 20 to 100 nm were obtained, including binary oxides (e.g., Cu_2O, ZnO, Fe_2O_3, Bi_2O_3, TiO_2, Nb_2O_5), color pigments (e.g., $CoAl_2O_4$, Cr_2O_3, α-Fe_2O_3), and luminescent materials (e.g., Y_2O_3:Eu, $LaPO_4$:Ce,Tb).[5] Aiming at metal oxide nanoparticles (Figure 1), diethylene glycol (DEG) turned out to be most advantageous and combines several features: *i*) water-comparable solubility of simple metal-salt precursors, *ii*) high synthesis temperature (100-200 °C) to obtain crystalline nanoparticles, and *iii*) good colloidal stabilization of the as-prepared metal-

Journal of Inorganic and General Chemistry
ZAAC
Zeitschrift für anorganische und allgemeine Chemie

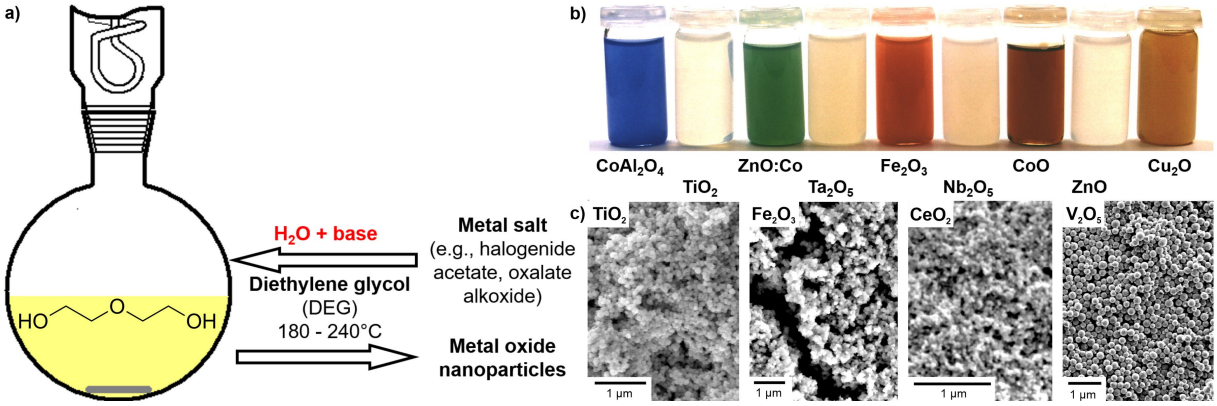

Figure 1. Polyol-mediated synthesis of different metal-oxide nanoparticles: a) scheme of synthesis, b) photos of suspensions of metal-oxide nanoparticles in DEG, c) electron microscopy of some examples (modified reproduction from[5a,b]).

oxide nanoparticles, optionally with simple removal of the polyol from the particle surface. In comparison to glycerol, DEG is less reducing, which promotes the formation of metal oxides. The *in situ* release of water due to the slow polymerization of DEG at high temperatures ($\geq 180\,^{\circ}C$) can be used to obtain small-sized nanoparticles, whereas larger nanoparticles require small portions of water in addition. In the course of understanding the polyol synthesis, finally, we also observed the formation of carbon dots (C-dots) via a controlled decomposition of polyols at high temperatures ($> 180\,^{\circ}C$).[6] Taken together, the polyol method in the meantime belongs to the standard repertoire for realizing metal nanoparticles and metal-oxide nanoparticles.[4,7]

Later on, we have focused the polyol synthesis on metal-molybdate and metal-tungstate nanoparticles and their photocatalytic properties.[8] Specifically, for β-$SnWO_4$ (Figure 2), nucleation and growth can be controlled and manipulated (e.g., by adjusting temperature, concentrations, way of precursor addition). Starting from the initial spherical nanoparticle, faceted microcrystals, including tetrahedra, star tetrahedra, truncated tetrahedra, truncated octahedra, cubes as well as the unique shape of spikecubes were obtained[8b] (Figure 2a). β-$SnWO_4$ nanoparticles, 20 nm in size, showed high biocompatibility as well as anti-tumor and anti-metastatic effects *in vitro* and *in vivo*, which is promising for photodynamic therapy (PDT) of near-surface tumors[8c] (Figure 2b). With the example of β-$SnWO_4$, moreover, a spikecube shape was shown for the first time and turned out to be interesting for photocatalysis[8b] (Figure 2c). Our photocatalytic studies also resulted in a peculiar $Au@Nb@H_xK_{1-x}NbO_3$ nanopeapod structure, which is suitable for photocatalytic water splitting with red/infrared light. Here, the biomimicry of the nanopeapod structure promotes near-field plasmon-plasmon coupling between bimetallic Au@Nb nanoantenna (the peas) and endows the UV-active $H_xK_{1-x}NbO_3$ semiconductor (the pods) with the ability to harvest VIS and NIR photons.[9]

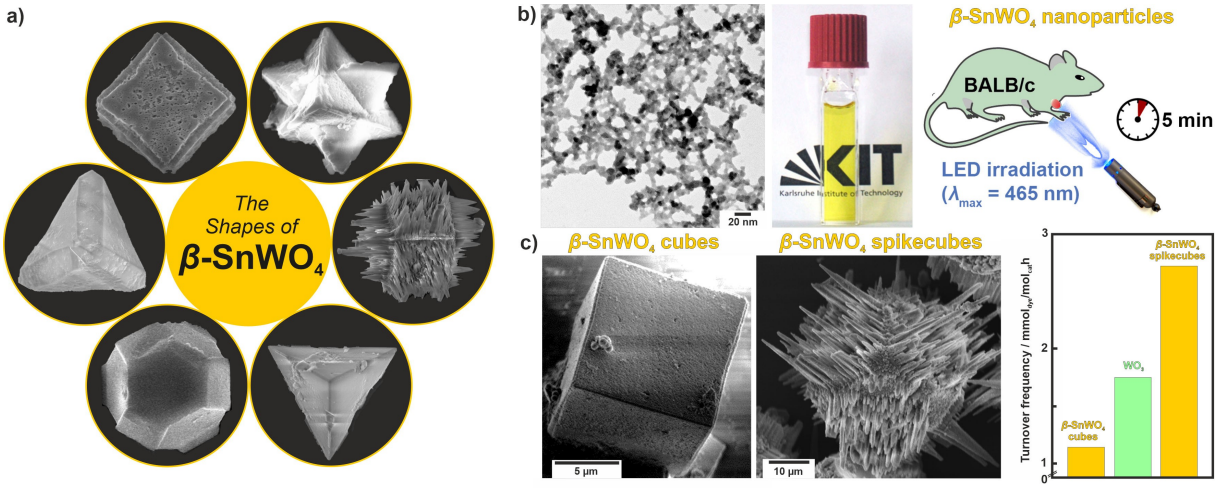

Figure 2. β-$SnWO_4$ with: a) different shapes, b) nanoparticles with TEM image and photo of aqueous suspension for photoactivated tumor treatment with blue-light excitation, c) photocatalytic degradation of rhodamine B with cube- and spikecube-type β-$SnWO_4$ with TEM images (modified reproduction from [8b,c]).

2.2. Microemulsions and hollow nanospheres

The micellar droplets of a thermodynamically stable microemulsion can be considered as nanoreactors being ideal for the synthesis of nanoparticles. Accordingly, microemulsions have been intensely used for the synthesis of a great number of nanoparticles.[10] Using microemulsion techniques, we could establish the synthesis of hollow nanospheres.[11] To obtain hollow nanospheres, the reactants are separately added to the polar droplet phase and to the non-polar dispersant phase, so that the precipitation of a solid is initiated at the liquid-to-liquid phase boundary of the microemulsion system (Figure 3a). With this synthesis strategy, hollow nanospheres of metal oxides (e.g., γ-AlO(OH), $La(OH)_3$, ZnO, Fe_2O_3, SnO_2, TiO_2, ZrO_2, $MgCO_3$, $Gd_2(CO_3)_3$), metal sulfides (e.g., CuS, $Cu_{1.8}S$, Cu_2S, Ag_2S) and elemental metals (Au, Ag) were obtained with outer diameters of 10–50 nm, a wall thickness of 2–10 nm, and an inner cavity ranging from 5 to 30 nm[11] (Figure 3b). In contrast to other approaches (e.g. hard-template methods[12]), microemulsions specifically allow to realize small-sized hollow nanospheres ($\leq$ 50 nm) with a size that directly correlates to the droplet size. Having the synthesis strategy and the hollow nanospheres available, their promising features for sensing, catalysis, and especially for drug delivery were studied as a next step.[13] Thus, $ZrO(HPO_4)$ or Fe_2O_3 hollow nanospheres filled with, for instance, cypermethrin, irinotecan, isoniazid, or benzothiazinone-043 show promising activity as insect repellant, anti-tumor agent, or for tuberculosis treatment.

Beside hollow nanospheres, we could show the existence and use of microemulsions with hydrogen peroxide and liquid ammonia as the droplet phase.[14] These microemulsions allowed the synthesis of BaO_2 nanoparticles (Figure 4a) or of Bi(0), Re(0), Fe(0), as well as of CoN and GaN nanoparticles with a mean diameter of 1–8 nm (Figure 4b). In regard of metal nanoparticles, liquid-ammonia microemulsions suffer from the fact that only $NaBH_4$ could be used as reducing agent, whereas, e.g., elemental sodium does dissolve with blue color but, thereafter, rapidly reacts with the surfactants. An interesting aspect, on the other hand, is that crystalline CoN and GaN were readily obtained at low temperature (−50 to +100 °C), which is unusual for metal nitrides prepared via conventional ammonolysis or nitridation and which typically requires considerably higher temperatures (> 400 °C).[15]

2.3. Base-metal nanoparticles and their reactivity

Although focused on metal oxides for a long time, we sometimes obtained metal nanoparticles via polyol synthesis or microemulsion synthesis (e.g., In(0), Bi(0), Re(0)[4d,14a]). This has triggered our interest in metal nanoparticles, and especially, the idea to prepare reactive base metals as nanoparticles in the liquid phase. This has resulted in different synthesis strategies, including the alkali-metal-driven reduction in liquid ammonia, the alkali-metal-naphthalenide-driven reduction in ethers, or the alkali-metal-pyridinyl-driven reduction in pyridine[16] (Fig-

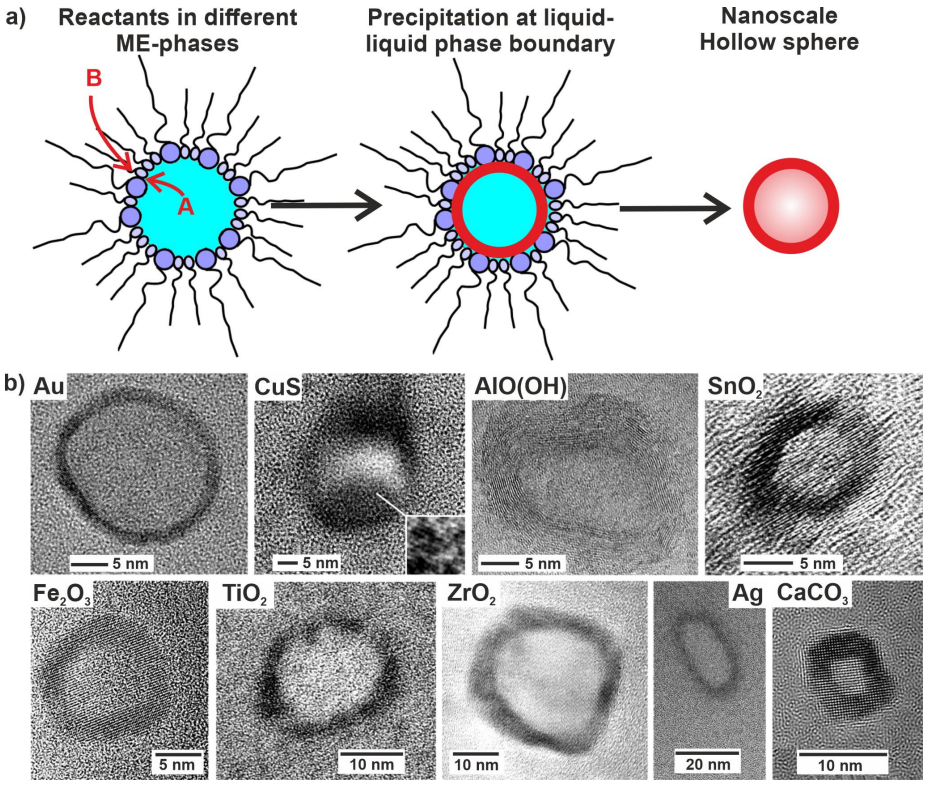

Figure 3. Hollow-nanosphere synthesis via microemulsion techniques: a) synthesis strategy and b) some examples of hollow nanospheres (modified reproduction from[11]).

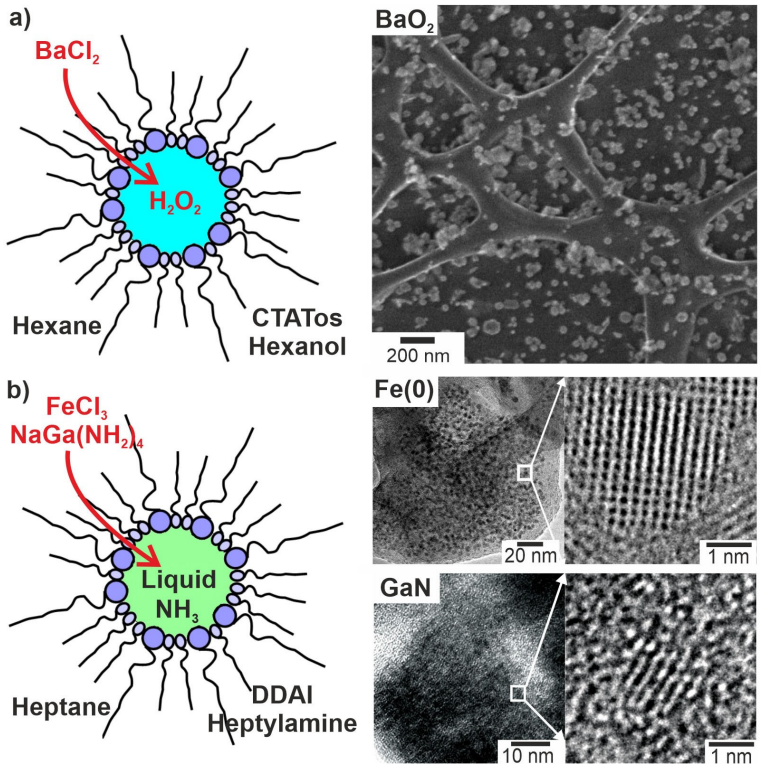

Figure 4. Microemulsions with a) hydrogen peroxide and b) liquid ammonia as the droplet phase and the herein prepared BaO_2, Fe(0) and GaN nanoparticles (CTATos: hexadecyltrimethylammonium-p-toluenesulfonate, DDAI: dimethyldioctylammonium iodide; modified reproduction from[14]).

ure 5). All these methods, of course, have their specific pros and cons. By now, all red-marked metals indicated in Figure 6 can be prepared in the liquid phase with diameters of 1–10 nm.[16] Especially those metals with electrochemical potentials (of the bulk metal) of −2.5 to −1.5 V – to the best of our knowledge – are hardly or even not available as nanoparticles until now. The challenge and difficulty can be exemplarily illustrated with Gd(0) nanoparticles. Here, the only reliable liquid-phase synthesis relates to the reduction of $GdCl_3$ with crown-ether-stabilized alkalides as powerful reducing agents.[17] Due to the high reactivity of the Gd(0) nanoparticles, they could only be identified as Gd_2O_3 via electron microscopy, or they need to be

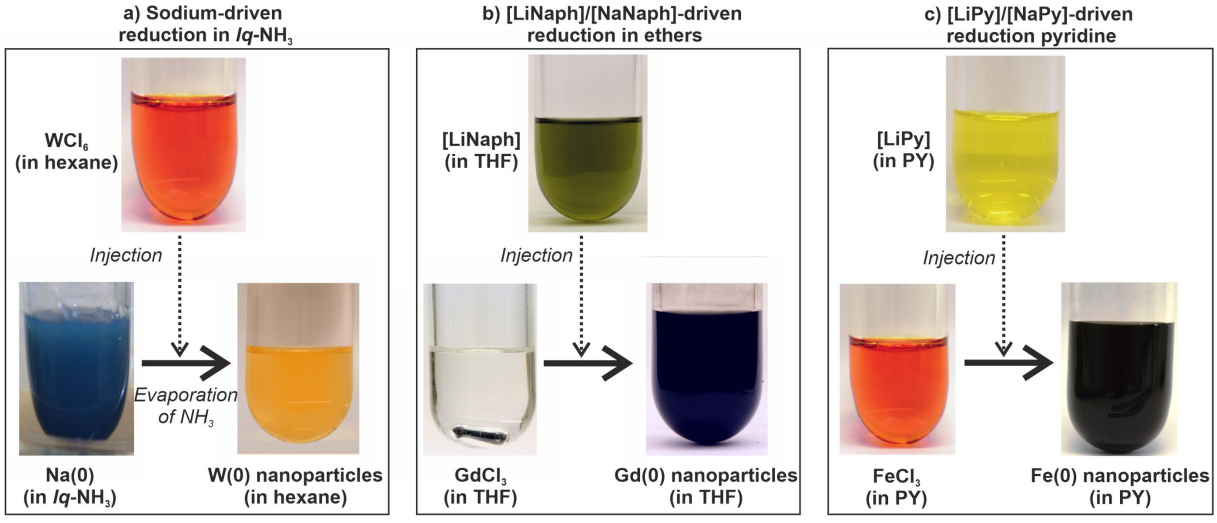

Figure 5. Synthesis strategies to obtain base-metal nanoparticles: a) alkali-metal-driven reduction in liquid ammonia, b) alkali-metal-naphthalenide-driven reduction in ethers, c) alkali-metal-pyridinyl-driven reduction in pyridine (modified reproduction from[16]).

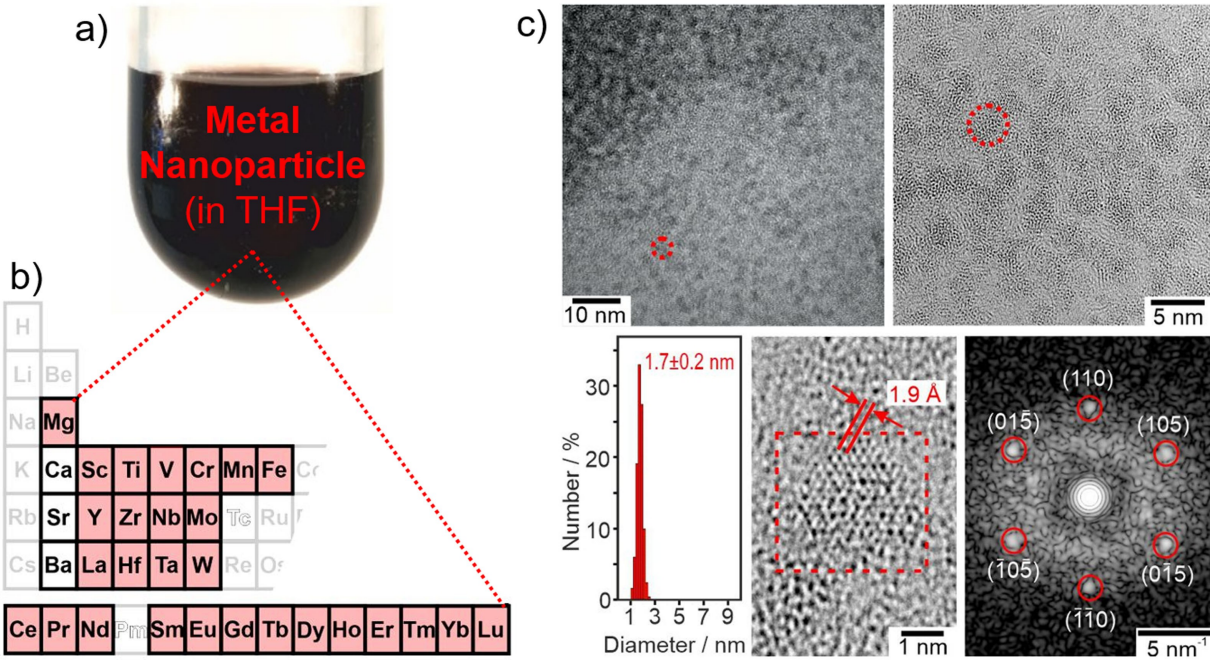

Figure 6. Liquid-phase synthesis of base-metal nanoparticles: a) suspension of metal nanoparticles in THF, b) red-marked metals available with the aforementioned synthesis strategies, c) electron microscopic characterization of base-metal nanoparticles with Sm(0) as specific example (modified reproduction from[16d]).

protected with a dense gold shell to result in Gd@Au core-shell nanoparticles. In fact, the challenge of reactive base-metal nanoparticles is not only related to the synthesis but also includes all handling and analytic characterization, which need to be performed under strict inert conditions (e.g., high-power centrifugation in gloveboxes, special transfer tools for all analytical equipment).

Since the alkali-metal-naphthalenide-driven reduction in ethers turned out to be specifically advantageous to prepare base-metal nanoparticles, we have also examined the chemical and thermal stability of alkali-metal naphthalenides in regard of the type of the alkali metal ([LiNaph], [NaNaph]), the type of the solvent (THF, DME), the temperature (–30 to +50 °C), and the time of storage (0 to 12 hours).[18] Although well-known and widely applied as powerful reducing agents,[19] the knowledge on the stability of alkali-metal naphthalenides was surprisingly limited. In inorganic synthesis, for instance, alkali-metal naphthalenides were used in main-group chemistry to establish element-element multiple bonds (e.g. B≡B) or to realize low-valence compounds (e.g., stannylenes, germylenes).[20] Alkali metal naphthalenides were also already used to prepare nanoparticles of zero-valent main-group elements (e.g., B, Si, Ge)[21] and transition metals (e.g., Co, Cu, Pd, Pt, Pt_3Sn, Bi, Ag, Au).[22] Based on a quantification via UV-Vis spectroscopy and by using the Lambert-Beer law, solutions of [LiNaph] in THF at low temperature turned out to be most stable. The decomposition of the naphthalenides could be related to a reductive polymerization of the solvent.[18]

Having all the reactive base-metal nanoparticles available since recently,[16d] their use as potential starting materials in follow-up reactions became an interesting question. Due to the small size of the base-metal nanoparticles, a high reactivity – even higher than for the respective bulk metals – can be expected. Another question is if the follow-up reactions are dominated, if not deteriorated by the ingredients and remains of the initial nanoparticle synthesis (e.g., naphthalene, THF, pyridine, LiCl/NaCl). First of all, the reactivity was probed with conventional oxidizing agents such as O_2, S_8, I_2, H_2O, or C_2H_5OH.[16d] Especially powder samples of the nanosized metals show violent reactions with air or water, which are comparable or even more violent than known for bulk alkali metals. In the liquid phase under inert atmosphere, however, the reactivity and reactions can be well-controlled and, for instance, result in bimetallic nanoparticles as well as metal-oxide and metal-sulfide nanoparticles or single-crystalline metal iodides and metal alkoxides.[16b-d] Moreover, the base-metal nanoparticles offer the option to prepare coordination compounds in the liquid phase at mild conditions (20–100 °C) (Figure 7).

Some first examples comprise an infinite $_\infty{}^1[FeI_2(CH_3OH)_2]$ chain, the triphenylphosphane complex $[FeI_2(PPh_3)_2]$, the organometallic compound $[Fe(Cp^*)_2]$, or the multinuclear oxo clusters $[Tm_5O(C_3H_7O)_{13}]$ and $[Sm_6O_4(cbz)_{10}(thf)_6]\cdot 2\,C_7H_8$ (HCbz: carbazole),[16c,18] which were obtained by controlled oxidation of Fe(0), Tm(0), and Sm(0) nanoparticles in the liquid phase between 20 and 80 °C (Figure 7). Although these compounds are only very first examples, they show that base-metal nanoparticles are suitable starting materials to obtain new single-crystalline compounds via liquid-phase synthesis. Moreover, the products of the reactions do not necessarily contain any

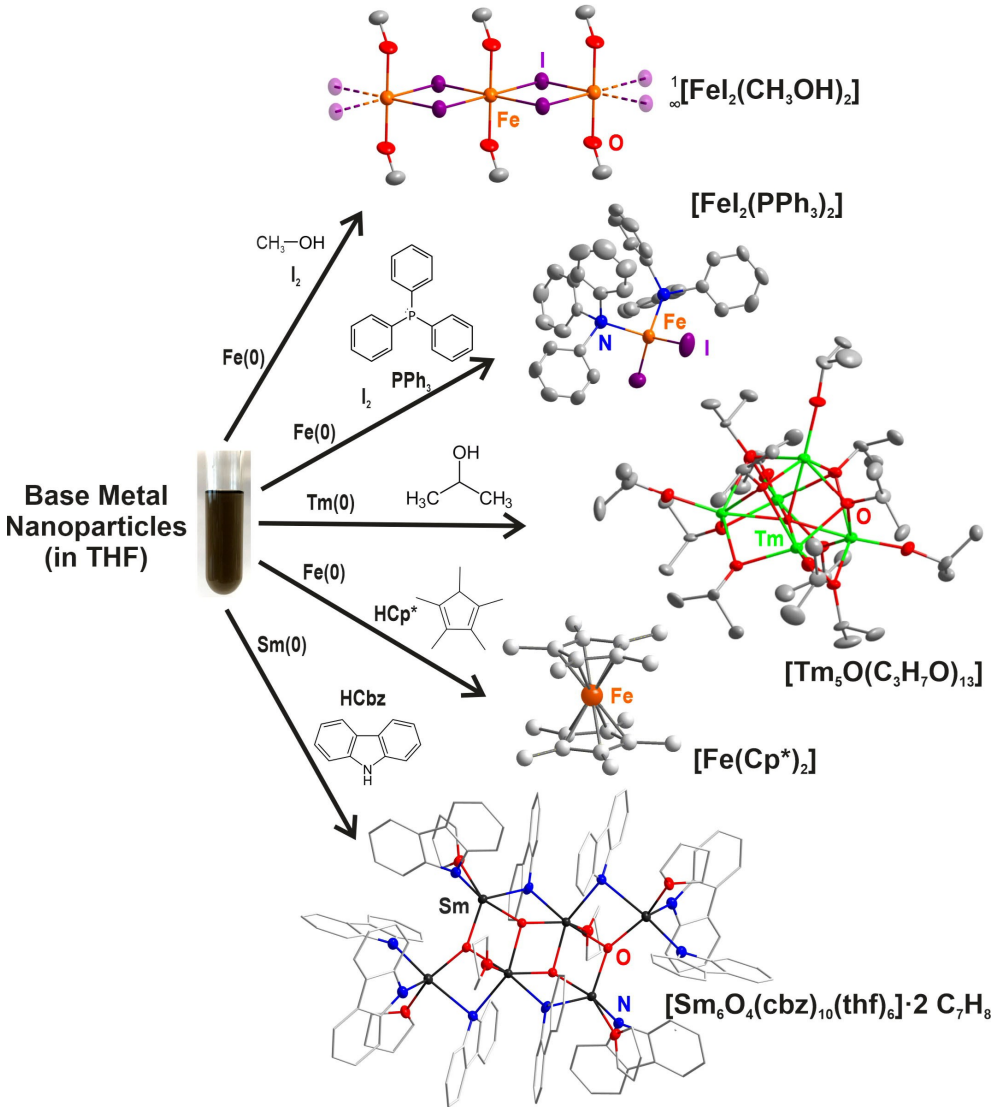

Figure 7. Exemplary coordination compounds and structures obtained by follow-up reactions using reactive base-metal nanoparticles as starting materials: $_\infty^1[FeI_2(CH_3OH)_2]$, $[FeI_2(PPh_3)_2]$, $[Tm_5O(C_3H_7O)_{13}]$, $[Fe(Cp^*)_2]$, and $[Sm_6O_4(cbz)_{10}(thf)_6]\cdot 2\ C_7H_8$ (H atoms omitted for clarity, modified reproduction from[16c,18]).

constituents of the initial base-metal-nanoparticle synthesis (e.g., naphthalene, THF, pyridine, LiCl/NaCl).

2.4. Ionic liquids, halogens and carbonyls

While searching for new liquid-phase syntheses, we were early fascinated by ionic liquids and their unique properties. Here, the weakly coordinating properties and the high redox stability seemed specifically interesting.[23] Inspired by the synthesis of nanoparticles in polyols, we have been starting with the synthesis of luminescent nanoparticles such as $LaPO_4$:Ce,Tb (10 ± 1 nm) and transparent conductive oxides such as In_2O_3:Sn (25 ± 3 nm) in ionic liquids (Figure 8), which are featured by high quantum yields (70%) and good conductivities ($3\pm3\times10^{-2}\,\Omega$cm).[24] Very recently, these studies on nanoparticles have been followed by GaN nanoparticles, which instantaneously after the ionic-liquid-based synthesis are monocrystalline, 3–8 nm in diameter, and exhibit a quantum yield of 55%.[24c]

Beside nanoparticles, however, our impression was that ionic liquids can be even more promising for the handling of reactive starting materials and the synthesis of novel compounds. After certain learning curve – for instance, on the thermal and chemical stability of ionic liquids, the way to grow single crystals, or the separation of the ionic liquid from the product after the synthesis – we have been focusing on polyhalides and halogen-rich metal halides as well as on carbonyl and cluster compounds. Some results, for instance, comprise the three-dimensional polybromide with $[C_4MPyr]_2[Br_{20}]$ (:[C_4MPyr] *N*-Butyl-*N*-methylpyrrolidinium) as well as further polyhalides (e.g., $[(Ph)_3PBr][Br_7]$, $[(Bz)(Ph)_3P]_2[Br_8]$, $[(n\text{-}Bu)_3MeN]_2[Br_{20}]$, $[(Ph)_3PCl]_2[Cl_2I_{14}]$, $[PBr_4][IBr_2]$) or bromine-con-

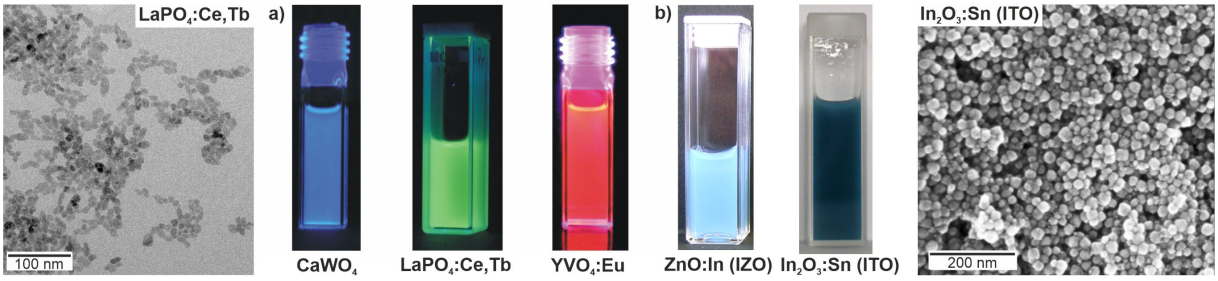

Figure 8. Ionic-liquid-based synthesis of a) luminescent nanomaterials and b) TCO nanomaterials (modified reproduction from[24a,b]).

taining bromidozincates such as $Zn_6Br_{12}(18\text{-crown-6})_2\times(Br_2)_5$[25] (Figure 9a). Aiming at carbonyl and cluster compounds, a $Ge_{12}Fe_8$ cluster core in $[Ge_{12}(\mu\text{-I})_4\{Fe(CO)_3\}_8]$, the carbonyl cation $[SnI_8\{Fe(CO)_4\}_4]^{2+}$ with a high-coordinated fragile $Sn^{+II}I_8$ unit, or the first bimetallic adamantane-like cluster core with Fe_4Sn_6 in $[BMIm]_2[\{Fe(CO)_3\}_4Sn_6I_{10}]$ were obtained[26] (Figure 9b).

While working with metal halides, recently, crown-ether-coordinated metal halides were obtained, which – to our surprise – showed unique luminescence properties.[27] Thus, rare Zn^{2+}-based fluorescence was observed and is unexpectedly efficient for ZnI_2(18-crown-6) with a quantum yield of 54%. Unprecedented quantum yields were observed for Mn_3I_6(18-crown-6)$_2$, $EuBr_2$(18-crown-6), and EuI_2(18-crown-6) with 98, 72, and 82%, respectively. Most remarkable, Mn_2I_4(18-crown-6) shows extremely strong emission with a quantum yield of 100%, anisotropic angle-dependent emission under polarized light, and second-harmonic generation (SHG). Due to the strong SHG intensity and the outstanding quantum yield, Mn_2I_4(18-crown-6) is also able to convert 1160–1280 nm light via virtual 580–640 nm light (due to the SHG effect) to orange emission peaking at 605 nm (due to the photoluminescence process). Such a situation is rare and promising for optoelectronic applications. In all these cases, the optical properties can be directly correlated with the specific structural features of the respective compound.[27] In regard to the synthesis, ionic liquids were the key to obtain all these compounds, which is related to the high stability, the weakly coordinating properties, and/or the reduced vapor pressure of, e.g., halogens and carbon monoxide over the ionic liquid. In sum, ionic-liquid-based synthesis has resulted in a great number of fascinating compounds in many research groups, including, for instance, the polychloride $[Et_4N]_2[(Cl_3)_2{\cdot}Cl_2]$, the intermetalloid $[CuBi_8]^{3+}$ cluster cation in $[CuBi_8][AlCl_4]_2[Al_2Cl_7]$, the heavy-metal porphyrin-analogue $[Hg_4Te_8(Te_2)_4]^{8-}$ in $[DMIm]_8[Hg_4Te_8(Te_2)_4]$ ($[DMIm]^+$: 1-decyl-3-methylimidazolium), the ligand-stabilized $[Ga_5]^{5+}$ pentagon, or complexes with a linear [N≡U≡N] core.[28] This impressively points to the unique role and properties of ionic liquids in inorganic chemistry.

2.5. Inorganic-organic hybrid nanoparticles and drug delivery

Based on the experience with industrial bulk phosphors for lamp and display applications, we were inspired by the biomedical use of fluorescent nanoparticles.[29] Beside organic,

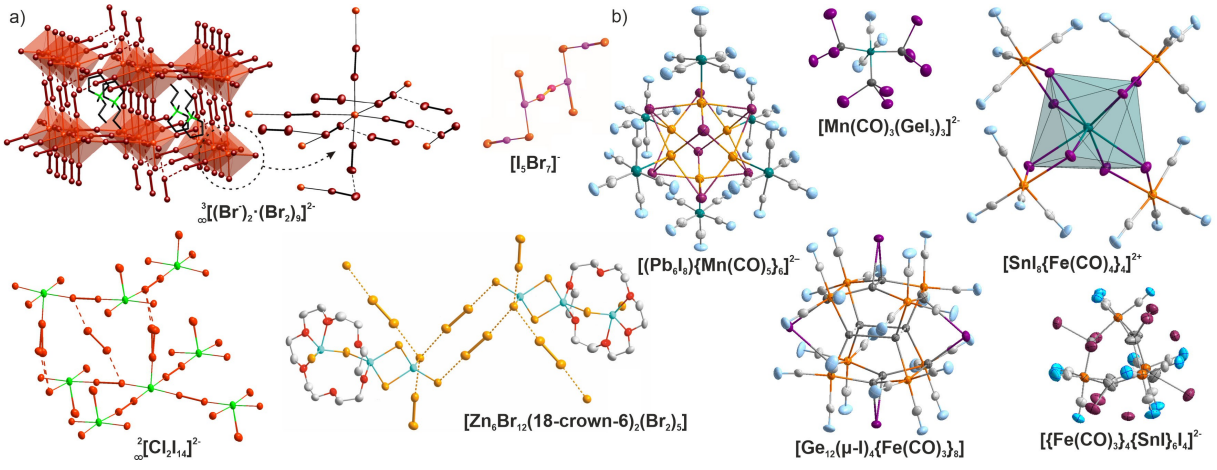

Figure 9. Ionic-liquid-based synthesis of new compounds with halogens and carbonyls as starting materials: a) polyhalides and halogen-rich metal halides and b) carbonyl and cluster compounds (modified reproduction from[25,26]).

molecular fluorophores and polymer-based nanoparticles, semiconductor-type quantum dots (e.g. CdSe@ZnS),[30] up-converting nanoparticles ($NaYF_4$:Er,Yb),[31] and dye-containing silica nanoparticles[32] are the domain of inorganic materials. In comparison to organic fluorophores, inorganic nanoparticles have the advantage of a significantly higher thermal, chemical, and photochemical stability, but they often suffer from higher toxicity (e.g. CdSe) and/or lower biocompatibility (e.g. due to slow body clearance). In regard of the specific requirements of biomedical applications, we intended to realize nanoparticles with simple composition and biocompatible constituents as well as a synthesis strictly limited to water.

With this aim, the concept of inorganic-organic hybrid nanoparticles (IOH-NPs) was developed.[33] Basically IOH-NPs have a composition $[M]^{n+}[R_{dye}SO_3]^-_n$, $[M]^{n+}[R_{dye}OPO_3]^{2-}_{n/2}$, or $[M]^{n+}[R_{drug}OPO_3]^{2-}_{n/2}$ with an inorganic cation (e.g., $[ZrO]^{2+}$, $[Gd(OH)]^{2+}$, $[Bi(OH)]^{2+}$) and a dye or drug anion $[R_{dye}SO_3]^-$, $[R_{dye}OPO_3]^{2-}$ or $[R_{drug}OPO_3]^{2-}$. Herein, the inorganic cation guarantees the insolubility of the IOH-NPs in water and, thus, allows the nucleation of nanoparticles. Due to the saline composition with equimolar amounts of inorganic cation and dye/drug anion, the IOH-NPs contain unprecedented high dye/drug loads of 70–85 wt-% per nanoparticle. Specific examples with fluorescent anions are, for instance, $[Gd(OH)]^{2+}{}_2[DB71]^{4-}$, $[ZrO]^{2+}[FMN]^{2-}$, $[GdO]^+[ICG]^-$, or $[Gd(OH)]^{2+}{}_2[EB]^{4-}$ (with DB71: direct blue 71, FMN: flavinmononucleotide, ICG: indocyanine green, EB: Evans blue) showing blue, green, red, or infrared emission, respectively (Figure 10a).[33] Beside the high dye-load, the IOH-NPs are characterized by a high photochemical stability, intense emission, and high cell uptake at low toxicity. Moreover, IOH-NPs such as $[GdO]^+[ICG]^-$ are suitable for multimodal imaging, including optical imaging (OI) due to the deep red emission of ICG, photoacoustic imaging (PAI) due to the wide and intense absorption of ICG, and magnetic resonance imaging (MRI) due to the paramagnetism of Gd^{3+}[33b] (Figure 10b).

The IOH-NPs are dissolved due to the normal metabolic activity of living cells and organisms over 1–4 days, which is advantageous for biomedical application in terms of biocompatibility and body clearance. Beside fluorescence labelling and imaging, this also offers the option to use IOH-NPs for drug delivery with different drugs as anions. Here, specific examples are, for instance, $[ZrO]^{2+}[(BMP)_{0.99}(DUT)_{0.01}]^{2-}$, $[ZrO]^{2+}[(CLP)_{0.99}(DUT)_{0.01}]^{2-}$, or $[ZrO]^{2+}[(FdUMP)_{0.99}(DUT)_{0.01}]^{2-}$ with the anti-inflammatory agent betamethasone phosphate (BMP), the last-line antibiotic clindamycin phosphate (CLP) or the chemotherapeutic agent 5′-fluoro-2′-deoxyuridine 5′-monophosphate (FdUMP)[33d,34] (Figure 11). These drug-containing IOH-NPs can of course as well contain small amounts of a fluorescent dye (0.005-5.0 mol-%) such as the deep-red emitting DYOMICS-647 uridine triphosphate. In the meantime, the IOH-NP concept has been expanded to >50 different drug anions, which are part of various cooperation's in biology and medicine.

3. Conclusion

On a journey, you never know what you'll find along the way – around the next bend, behind the next knoll. This is all the more true for scientific paths with their aberrations, dead ends, and surprises. Time and again, experimental chemistry has been frustrating and at the same time most exciting when an experiment did not lead to the expected but to a much more interesting result than originally thought. Based on different liquid-phase syntheses (including water, polyols, ethers, liquid ammonia, ionic liquids) and different types of compounds (including metal-oxide nanoparticles, base-metal nanoparticles, hollow nanospheres, polyhalides and halogen-rich metal halides, carbonyl and cluster compounds, inorganic-organic hybrid nanoparticles), a result from one topic often also turned out to be useful for another topic and question. After about 20 years of our journey through inorganic chemistry with *"large"* solids (single-crystalline compounds) and *"small"* solids (nanomaterials) is science all the more fascinating and full of surprises. In fact, science never ends, but continually reinvents itself by emerging new questions. In this sense, we wish the journal

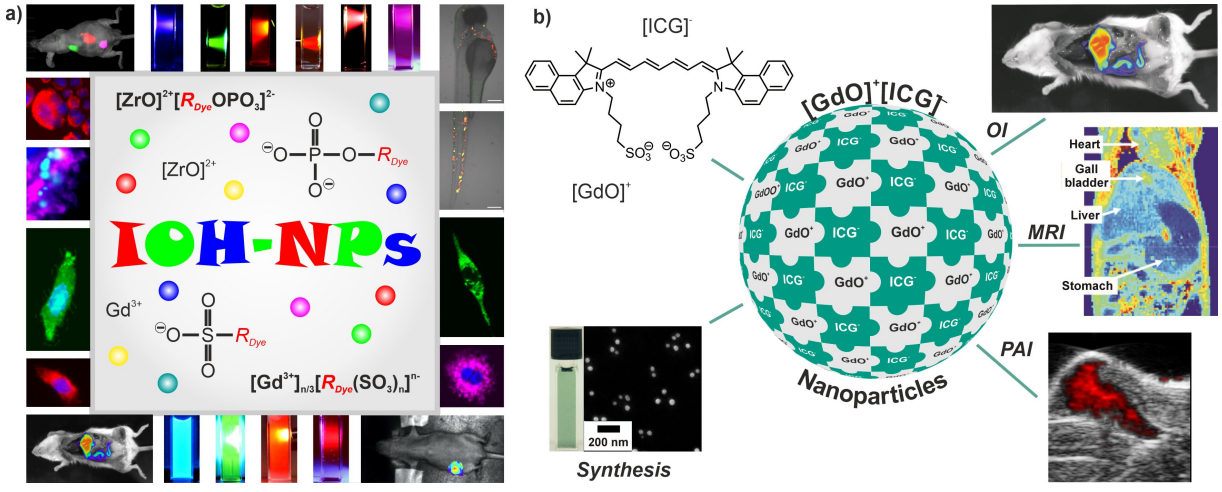

Figure 10. IOH-NPs with a) different emission color and b) options for multimodal imaging (modified reproduction from[33a,d]).

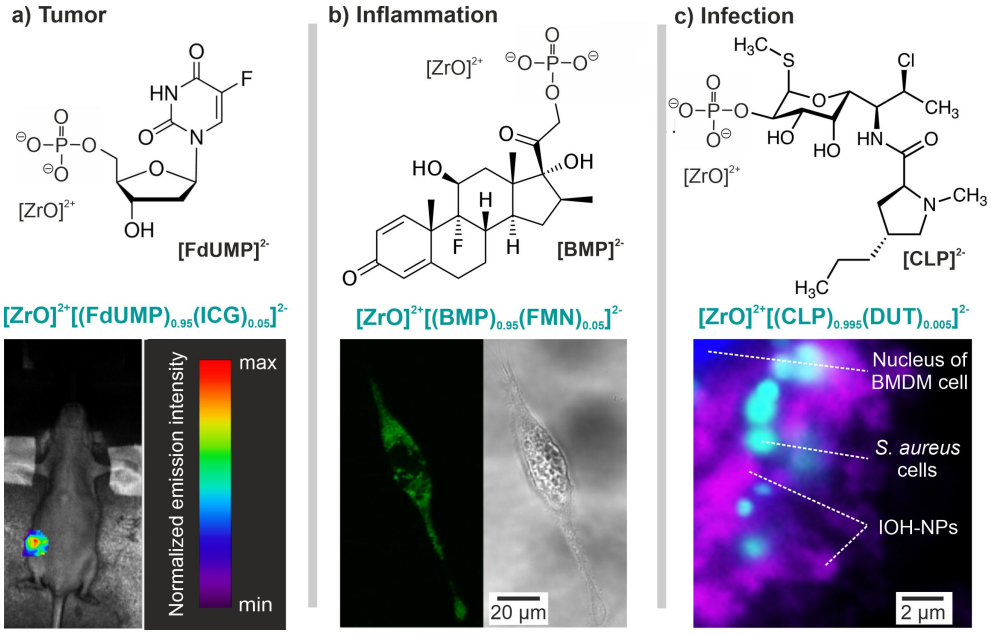

Figure 11. IOH-NPs for drug delivery with different types of drug anions and examples from biomedical studies related to a) tumors, b) inflammation, c) infection (modified reproduction from[33d,34]).

another successful 130 years with fascinating research, results, and compounds in inorganic chemistry!

Acknowledgements

The author, first of all, acknowledges all PostDocs, PhDs, master and bachelor students who worked on all the aforementioned compounds and materials as well as the permanent staff of the group and the institute for excellent collaboration, specifically including Anette Baust and Dr. Silke Wolf. I also owe a great debt of gratitude to all the partners and colleagues from chemistry, physics, engineering, biology, and medicine for many years of trusting cooperation. Especially, I like to thank Professor Dagmar Gerthsen, Laboratory for Electron Microscopy (KIT), and Professor Frauke Alves, Max-Planck-Institute for Experimental Medicine (Göttingen), for all the support and the discussions on electron microscopy and nanoparticles in medicine. Finally, I am grateful for those organizations who provided funding and equipment, and among them especially the Deutsche Forschungsgemeinschaft (DFG). Open Access funding enabled and organized by Projekt DEAL.

Conflict of Interest

The authors declare no conflict of interest.

Data Availability Statement

The data that support the findings of this study are available from the corresponding author upon reasonable request.

Keywords: Base-metal nanoparticles · hollow nanospheres · cluster compounds · inorganic-organic hybrid nanoparticles

[1] M. Jansen, C. Feldmann, W. Müller, *Z. Anorg. Allg. Chem.* **1992**, *611*, 7–10.
[2] C. Feldmann, *Z. Anorg. Allg. Chem.* **2004**, *630*, 2473–2477.
[3] F. Fievet, J. P. Lagier, M. Figlarz, *MRS Bull.* **1989**, 29–34.
[4] a) S. Ammar, F. Fievet, *Nanomater.* **2020**, *10*, 1217; b) F. Fievet, S. Ammar-Merah, R. Brayner, F. Chau, M. Giraud, F. Mammeri, J. Peron, J.-Y. Piquemal, L. Sicard, G. Viau, *Chem. Soc. Rev.* **2018**, *47*, 5187–5233; c) Y. Chen, Z. Fan, Z. Zhang, W. Niu, C. Li, N. Yang, B. Chen, H. Zhang, *Chem. Rev.* **2018**, *118*, 6409–6455; d) H. Dong, Y.-C. Chen, C. Feldmann, *Green Chem.* **2015**, *17*, 4107–4132.
[5] a) C. Feldmann, H. O. Jungk, *Angew. Chem. Int. Ed.* **2001**, *40*, 359–362; *Angew. Chem.* **2001**, *113*, 372–374; b) C. Feldmann, *Adv. Funct. Mater.* **2003**, *13*, 101–107; c) P. Schmitt, N. Brem, S. Schunk, C. Feldmann, *Adv. Funct. Mater.* **2011**, *21*, 3037–3046.
[6] a) H. Dong, A. Kuzmanoski, D. M. Gößl, R. Popescu, D. Gerthsen, C. Feldmann, *Chem. Commun.* **2014**, *50*, 7503–7506; b) H. Dong, M. Roming, C. Feldmann, *Part. Part. Syst. Charact.* **2015**, *32*, 467–475.
[7] a) H. Kaneko, T. Matsumoto, J. L. Cuya Huaman, M. Ishijima, K. Suzuki, H. Miyamura, J. Balachandran, *Inorg. Chem.* **2021**, *60*, 3025–3036; b) D. Wu, K. Kusada, T. Yamamoto, T. Toriyama, S. Matsumura, I. Gueye, O. Seo, J. Kim, S. Hiroi, O. Sakata, S. Kawaguchi, Y. Kubota, H. Kitagawa, *Chem. Sci.* **2020**, *11*, 12731–12736; c) Z. Chen, T. Balankura, K. A. Fichthorn, R. M. Rioux, *ACS Nano* **2019**, *13*, 1849–1860; d) R. K. Ramamoorthy,

A. Viola, B. Grindi, J. Peron, C. Gatel, M. Hytch, R. Arenal, L. Sicard, M. Giraud, J.-Y. Piquemal, G. Viau, *Nano Lett.* **2019**, *19*, 9160–9169; e) J. Teichert, M. Ruck, *Europ. J. Inorg. Chem.* **2019**, 2267–2276.

[8] a) J. Ungelenk, C. Seidl, E. Zittel, S. Roming, U. Schepers, C. Feldmann, *Chem. Commun.* **2014**, *50*, 6600–6603; b) Y.-C. Chen, Y.-G. Lin, L.-C. Hsu, A. Tarasov, P.-T. Chen, M. Hayashi, J. Ungelenk, Y.-K. Hsu, C. Feldmann, *ACS Catal.* **2016**, *6*, 2357–2367; c) C. Seidl, J. Ungelenk, E. Zittel, T. Bergfeldt, J. P. Sleeman, U. Schepers, C. Feldmann, *ACS Nano* **2016**, *10*, 3149–3157.

[9] Y.-C. Chen, Y.-K. Hsu, R. Popescu, D. Gerthsen, Y.-G. Lin, C. Feldmann, *Nat. Commun.* **2018**, *9*, 232(1-11).

[10] a) A. K. Ganguli, A. Ganguly, S. Vaidya, *Chem. Soc. Rev.* **2010**, *39*, 474–485; b) M. P. Pileni, *J. Phys. Chem.* **1993**, *97*, 6961–6973.

[11] a) C. Zimmermann, C. Feldmann, M. Wanner, D. Gerthsen, *Small* **2007**, *3*, 1347–1349; b) H. Gröger, F. Gyger, P. Leidinger, C. Zurmühl, C. Feldmann, *Adv. Mater.* **2009**, *21*, 1586–1590; c) S. Wolf, C. Feldmann, *Angew. Chem. Int. Ed.* **2016**, *55*, 15728–15752; *Angew. Chem.* **2016**, *128*, 15958–15984; d) M. Liebertseder, D. Wang, G. Cavusoglu, M. Casapu, S. Wang, S. Behrens, C. Kübel, J.-D. Grunwaldt, C. Feldmann, *Nanoscale* **2021**, *13*, 2005–2011.

[12] a) X. Wang, J. Feng, Y. Bai, Q. Zhang, Y. Yin, *Chem. Rev.* **2016**, *116*, 10983–11060; b) X. W. Lou, Z. Archer, Z. Yang, *Adv. Mater.* *20*, 3987–4019.

[13] a) P. Leidinger, J. Treptow, K. Hagens, J. Eich, N. Zehethofer, D. Schwudke, W. Öhlmann, H. Lünsdorf, O. Goldmann, U. E. Schaible, K. E. J. Dittmar, C. Feldmann, *Angew. Chem. Int. Ed.* **2015**, *54*, 12597–12601; *Angew. Chem.* **2015**, *127*, 12786–12791; b) V. Rein, E. Zittel, K. Hagens, N. Redinger, U. Schepers, H. Mehlhorn, U. Schaible, C. Feldmann, *Adv. Funct. Mater.* **2019**, *29*, 1900543.

[14] a) F. Gyger, P. Bockstaller, D. Gerthsen, C. Feldmann, *Angew. Chem. Int. Ed.* **2013**, *52*, 12443–12447; *Angew. Chem.* **2013**, *125*, 12671–12675; b) R. Gomes, S. Roming, A. Przybilla, M. A. R. Meier, C. Feldmann, *J. Mater. Chem. C* **2014**, *2*, 1513–1518.

[15] a) R. E. Karaballi, Y. E. Monfared, M. Dasog, *Chem. Eur. J.* **2020**, *26*, 8499–8505; b) T. M. M. Richter, R. Niewa, *Inorganics* **2014**, *2*, 29–78; c) L. Xu, S. Li, Y. Zhang, Y. Zhai, *Nanoscale* **2012**, *4*, 4900–4915; d) C. Giordano, M. Antonietti, *Nano Today* **2011**, *6*, 366–380.

[16] a) C. Schöttle, P. Bockstaller, D. Gerthsen, C. Feldmann, *Chem. Commun.* **2014**, *50*, 4547–4550; b) C. Schöttle, P. Bockstaller, R. Popescu, D. Gerthsen, C. Feldmann, *Angew. Chem. Int. Ed.* **2015**, *54*, 9866–9870; *Angew. Chem.* **2015**, *127*, 10004–10008; c) A. Egeberg, T. Block, O. Janka, O. Wenzel, D. Gerthsen, R. Pöttgen, C. Feldmann, *Small* **2019**, *15*, 1902321(1-9); d) D. Bartenbach, O. Wenzel, R. Popescu, L.-P. Faden, A. Reiß, M. Kaiser, A. Zimina, J.-D. Grunwaldt, D. Gerthsen, C. Feldmann, *Angew. Chem. Int. Ed.* **2021**, *60*, 17373–17377.

[17] a) J. A. Nelson, L. H. Bennet, J. J. Wagner, *J. Am. Chem. Soc.* **2002**, *124*, 2979–2983; b) C. Yan, M. J. Wagner, *Nano Lett.* **2013**, *13*, 2611–2614.

[18] A. Reiß, C. Donsbach, C. Feldmann, *Dalton Trans.* **2021**, *50*, 16343–16352.

[19] N. G. Connelly, W. E. Geiger, *Chem. Rev.* **1996**, *96*, 877–910.

[20] a) C. Mohapatra, L. T. Scharf, T. Scherpf, B Mallick, K.-S. Feichtner, C. Schwarz, V. H. Gessner, *Angew. Chem. Int. Ed.* **2019**, *58*, 7459–7463; *Angew. Chem.* **2019**, *131*, 7537–7541; b) S. Morisako, R. Shang, Y. Yamamoto, H. Matsui, M. Nakano, *Angew. Chem. Int. Ed.* **2017**, *56*, 15234–15240; *Angew. Chem.* **2017**, *129*, 15436–15442; c) H. Braunschweig, H. D. Dewhurst, K. Hammond, J. Mies, K. Radacki, A. Vargas, *Science* **2012**, *336*, 1420–1422; d) W. D. Woodul, E. Carter, R. Mîller, A. F. Richards, A. Stasch, M. Kaupp, D. M. Murphy, M. Driess, C. Jones, *J. Am. Chem. Soc.* **2011**, *133*, 10074–10077; e) K. Suzuki, T. Matsuo, D. Hashizume, H. Fueno, K. Tanaka, K. Tamao, *Science* **2011**, *331*, 1306–1309; f) R. C. Fischer, P. P. Power, *Chem. Rev.* **2010**, *110*, 3877–3923; g) R. E. Jilek, M. Jang, E. D. Smolensky, D. J. Britton, J. E. Ellis, *Angew. Chem. Int. Ed.* **2008**, *47*, 8692–8695; *Angew. Chem.* **2008**, *120*, 8820–8823; h) W. W. Brennessel, V. G. Young, J. E. Ellis, *Angew. Chem. Int. Ed.* **2006**, *45*, 7426–7429.

[21] a) S. Yao, A. Kostenko, Y. Xiong, A. Ruzicka, M. Driess, *J. Am. Chem. Soc.* **2020**, *142*, 12608–12612; b) A. L. Pickering, C. Mitterbauer, N. D. Browning, S. M. Kauzlarich, P. P. Power, *Chem. Commun.* **2007**, 580–582; c) H. W. Chiu, C. N. Chervin, S. M. Kauzlarich, *Chem. Mater.* **2005**, *17*, 4858–4864.

[22] a) X. Chen, H. Cao, X. Chen, Y. Du, J. Qi, J. Luo, M. Armbrüster, C. Liang, *ACS Appl. Mater. Interfaces* **2020**, *12*, 18551–18561; b) F. Fu, A. M. Martinez-Villacorta, A. Escobar, J. Irigoyen, S. Moya, E. Fouquet, J. Ruiz, D. Astruc, *Inorg. Chem. Front.* **2017**, *4*, 2037–2044; c) M. Branca, K. Corp, D. Ciuculescu-Pradines, Y. Coppel, P. Lecante, C. Amiens, *New J. Chem.* **2017**, *41*, 5960–5966; d) M. Schulz-Dobrick, K. V. Sarathy, M. Jansen, *J. Am. Chem. Soc.* **2005**, *127*, 12816–12817.

[23] P. Wasserscheid, T. Welton, *Ionic Liquids in Synthesis*, Wiley-VCH, Weinheim **2008**.

[24] a) G. Bühler, C. Feldmann, *Angew. Chem. Int. Ed.* **2006**, *45*, 4864–4867; *Angew. Chem.* **2006**, *118*, 4982–4986; b) G. Bühler, D. Thölmann, C. Feldmann, *Adv. Mater.* **2007**, *19*, 2224–2227; c) H. F. Gaiser, R. Popescu, D. Gerthsen, C. Feldmann, *Chem. Commun.* **2020**, *56*, 2312–2315.

[25] a) M. Wolff, J. Meyer, C. Feldmann, *Angew. Chem. Int. Ed.* **2011**, *50*, 4970–4973; *Angew. Chem.* **2011**, *123*, 5073–5077; b) M. Wolff, A. Okrut, C. Feldmann *Inorg. Chem.* **2011**, *50*, 11683–11694; c) D. Hausmann, C. Feldmann, *Inorg. Chem.* **2016**, *55*, 6141–6147.

[26] a) S. Wolf, K. Reiter, F. Weigend, W. Klopper, C. Feldmann, *Inorg. Chem.* **2015**, *54*, 3989–3994; b) S. Wolf, W. Klopper, C. Feldmann, *Chem. Commun.* **2018**, *54*, 1217–1220; c) S. Wolf, R. Köppe, T. Block, R. Pöttgen, P. W. Roesky, C. Feldmann, *Angew. Chem. Int. Ed.* **2020**, *59*, 5510–5514; *Angew. Chem.* **2020**, *132*, 5552–5556.

[27] E. Merzlyakova, S. Wolf, S. Lebedkin, L. Bayarjargal, B. L. Neumeier, D. Bartenbach, C. Holzer, W. Klopper, B. Winkler, M. Kappes, C. Feldmann, *J. Am. Chem. Soc.* **2021**, *143*, 798–804.

[28] a) T. Zhang, T. Doert, H. Wang, S. Zhang, M. Ruck, *Angew. Chem. Int. Ed.* **2021**, *60*, 22148–22165; b) R. Brueckner, H. Haller, S. Steinhauer, C. Mueller, S. A. Riedel, *Angew. Chem. Int. Ed.* **2015**, *54*, 15579–15583; *Angew. Chem.* **2015**, *127*, 15800–15804; c) M. Knies, M. Kaiser, A. Isaeva, U. Mueller, T. Doert, M. Ruck, *Chem. Eur. J.* **2018**, *24*, 127–132; d) C. Donsbach, K. Reiter, D. Sundholm, F. Weigend, S. Dehnen, *Angew. Chem. Int. Ed.* **2018**, *57*, 8770–8774; *Angew. Chem.* **2018**, *130*, 8906–8910; e) K. Glootz, D. Himmel, D. Kratzert, B. Butschke, H. Scherer, I. Krossing, *Angew. Chem. Int. Ed.* **2019**, *58*, 14162–14166; *Angew. Chem.* **2019**, *131*, 14300–14304; f) S. S. Rudel, H. L. Deubner, M. Mueller, A. J. Karttunen, F. Kraus, *Nat. Chem.* **2020**, *12*, 962–967.

[29] a) E. Ximendes, A. Benayas, D. Jaque, R. Marin, *ACS Nano* **2021**, *15*, 1917–1941; b) S. Kunjachan, J. Ehling, G. Storm, F. Kiessling, T. Lammers, *Chem. Rev.* **2015**, *115*, 10907–10937; c) O. S. Wolfbeis, *Chem. Soc. Rev.* **2015**, *44*, 4743–4768.

[30] a) K. D. Wegner, N. Hildebrandt, *Chem. Soc. Rev.* **2015**, *44*, 4792–4834; b) X. Michalet, F. F. Pinaud, L. A. Bentolila, J. M. Tsay, S. Doose, J. J. Li, G. Sundaresan, A. M. Wu, S. S. Gambhir, S. Weiss, *Science* **2005**, *307*, 538–544.

[31] a) G. Chen, H. Agren, T. Y. Ohulchanskyy, P. N. Prasad, *Chem. Soc. Rev.* **2015**, *44*, 1680–1713; b) M. Haase, H. Schaefer, *Angew. Chem. Int. Ed.* **2011**, *50*, 5808–5829; *Angew. Chem.* **2011**, *123*, 5928–5950.

[32] a) J. G. Croissant, K. S. Butler, J. I. Zink, C. J. Brinker, *Nature Rev. Mater.* **2020**, *5*, 886–909; b) C. Caltagirone, A. Bettoschi, A. Garau, R. Montis, *Chem. Soc. Rev.* **2015**, *44*, 4645–4671.

[33] a) M. Roming, H. Lünsdorf, K. E. J. Dittmar, C. Feldmann, *Angew. Chem. Int. Ed.* **2010**, *49*, 632–637; *Angew. Chem.* **2010**, *122*, 642–647; b) M. Poß, R. J. Tower, J. Napp, L. C. Appold, T. Lammers, F. Alves, C.-C. Glüer, S. Boretius, C. Feldmann, *Chem. Mater.* **2017**, *29*, 3547–3554; c) M. Poß, E. Zittel, C. Seidl, A. Meschkov, L. Muñoz, U. Schepers, C. Feldmann, *Adv. Funct. Mater.* **2018**, *28*, 1801074(1-8); d) B. L. Neumeier, M. Khorenko, F. Alves, O. Goldmann, J. Napp, U. Schepers, H. M. Reichardt, C. Feldmann, *ChemNanoMat* **2019**, *5*, 24–45.

[34] a) J. G. Heck, J. Napp, S. Simonato, J. Möllmer, M. Lange, H. R. Reichardt, R. Staudt, F. Alves, C. Feldmann, *J. Am. Chem. Soc.* **2015**, *137*, 7329–7336; b) J. Napp, M. A. Markus, J. G. Heck, C. Dullin, W. Möbius, D. Gorpas, C. Feldmann, F. Alves, *Theranostics* **2018**, *8*, 6367–6368.

Manuscript received: February 11, 2022
Revised manuscript received: March 17, 2022

RESEARCH ARTICLE

*Prof. Dr. C. Feldmann**